

Mantle structure and dynamic topography in the Mediterranean Basin

L. Boschi,¹ C. Faccenna,² and T. W. Becker³

Received 5 August 2010; revised 3 September 2010; accepted 8 September 2010; published 20 October 2010.

[1] We study the contribution of mantle flow to surface deformation within the Mediterranean Basin. Flow is modeled numerically based on lateral changes in mantle temperature estimated from tomography models. We find that modeling results are significantly affected by the properties of the selected tomography models. Shear-velocity models based on surface-wave observations achieve the highest resolution of upper-mantle structure, and, as a result, are most successful in predicting microplate motion and dynamic topography. **Citation:** Boschi, L., C. Faccenna, and T. W. Becker (2010), Mantle structure and dynamic topography in the Mediterranean Basin, *Geophys. Res. Lett.*, 37, L20303, doi:10.1029/2010GL045001.

1. Introduction

[2] The observed topography of the Earth's surface is explained by the combined effects of shallow processes like erosion or sedimentation, and deep ones like isostatic compensation and the upward push/downward pull associated with convective flow in the mantle [Gurnis, 2001]. The latter term, known as dynamic topography, has been evaluated in a number of studies, where models of mantle density are defined on the basis of seismic tomography, and used to predict the associated mantle flow [Forte, 2007]. The large-scale patterns of topography in western North America [Moucha *et al.*, 2008], southern Africa [Lithgow-Bertelloni and Silver, 1998] and Arabia [Daradich *et al.*, 2003], for example, have been explained in terms of whole-mantle convection.

[3] In regions where the resolution of tomography models is high, it is possible to model smaller scale, shallow (top few hundred km of the upper mantle) convection processes, accordingly explaining the shorter-wavelength component of topography. One example is the Mediterranean Basin, where mantle structure has been illuminated by a number of high-resolution tomography models. Observed plate velocity, seismicity and topography suggest that the region is composed of a mosaic of blocks that move independently from the overall convergence [Serpelloni *et al.*, 2007]: (i) the southern part of Adria, separated from the rest of the plate by the middle-Adriatic shear zone [Favali *et al.*, 1993; D'Agostino *et al.*, 2008], slowly moves eastward with

respect to Eurasia; (ii) in the same reference frame, Anatolia moves westward by ~ 2 cm/yr, while (iii) Aegea moves predominantly southward (~ 3 cm/yr) [Reilinger *et al.*, 2006]. Vertical motion in the area is, at least at some sites, as fast as the horizontal, as illustrated by holocene notches, marine terraces and karst caves along the southern Italian coast line [Ferranti *et al.*, 2006], the Hellenic arc and in Spain [Casas-Sainz and de Vicente, 2009]. The Anatolia-Iran highplain is also related to large-scale uplift, with less well constrained timing.

[4] Faccenna and Becker [2010, hereafter FB10] have shown that 3-D density heterogeneity and corresponding flow in the upper mantle can at least partially account for this complex pattern of horizontal and vertical motion. In the following we explore how different modeling results for microplate motion and topography throughout the Mediterranean basin are obtained on the basis of different tomography models. We find that shear-velocity models of the region provide a better fit of geophysical observables than achieved by the compressional-velocity ones. In addition, predictions of the horizontal and vertical motion of Iberia, Adria and Anatolia based on the new high-resolution models considered here are now more consistent with observations. This is a significant step to understand, in general, the style of convection beneath converging margins, and towards the identification of a consensus seismic model of the Mediterranean upper mantle.

2. Surface Deformation in the Mediterranean Region

[5] The Mediterranean region is a diffuse plate boundary where sharp topographic features and deformation are distributed on a wide area. We show in Figure 1 the difference between observed Earth's topography and its isostatic component, computed based on crustal densities and layer thicknesses from the global crustal model Crust2.0 [Bassin *et al.*, 2000] (Figure 1a), and from the regional crustal model Eurocrust07 of Tesauro *et al.* [2008] (Figure 1b), with densities again taken from Crust2.0. Both maps and model predictions are filtered by convolution with a 250 km-radius Gaussian function to eliminate artifacts related to gridding and to remove small-scale structure that is flexurally supported. This "residual" topography should approximately coincide with dynamic topography caused by mantle flow alone. In areas where Figures 1a and 1b differ (e.g., Anatolia), the more recent model Eurocrust07 (Figure 1b) should be taken as reference.

[6] Our set of geophysical observations is augmented by the plate velocities of Adria and Anatolia (GPS measurements reported by Serpelloni *et al.* [2007]), and Africa and

¹Institute of Geophysics, ETH, Zurich, Switzerland.

²Dipartimento di Scienze Geologiche, Università di Roma 3, Rome, Italy.

³Department of Earth Sciences, University of Southern California, Los Angeles, California, USA.

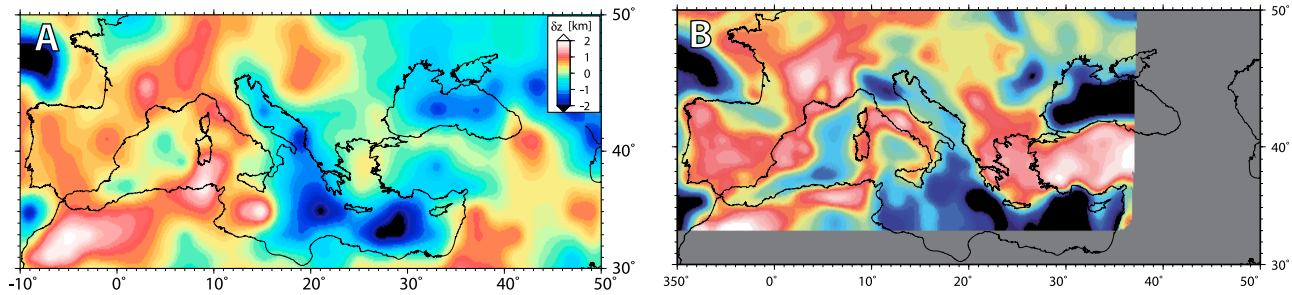


Figure 1. (a) Residual topography after correcting for isostatic adjustment based on the crustal model Crust2.0 [Bassin *et al.*, 2000]. (b) same as Figure 1a, isostatic adjustment computed from Eurocrust07 [Tesauro *et al.*, 2008], with density values taken, again, from Crust2.0.

Arabia (model NUVEL-1A by DeMets *et al.* [1990, 1994]), with respect to a fixed Eurasian plate.

3. Seismic Imaging of Mantle Structure

[7] FB10 employed a set of three tomographic models of the Earth's mantle as alternative input parameters of their mantle-flow models: the global P -velocity model of Li *et al.* [2008] (dubbed model MITP08 in the following); the Mediterranean upper mantle model of Piromallo and Morelli [2003] (PM01); the S -velocity upper-mantle model of Lebedev and van der Hilst [2008], merged with SMEAN [Becker and Boschi, 2002] in the lower mantle (LH08).

[8] PM01 and MITP08 are high-resolution models based on large travel-time databases, including phases that are particularly sensitive to regional-scale, upper-mantle structure; yet they were derived without making use of surface-wave observations, which provide a stronger constraint on uppermost mantle structure, but are almost only sensitive to S velocity. LH08 is based on observations of surface waves, but has by construction relatively low resolution of regional-scale structure.

[9] Here we additionally consider two S -velocity models that resolve short-scale length features under the Mediterranean Basin: the global, multiple-resolution model LRSP30EU of Boschi *et al.* [2009], based on teleseismic measurements of surface-wave phase velocities, and the regional model of Schmid *et al.* [2008], merged with S2ORTS [Ritsema *et al.*, 1999] outside the region of interest, obtained from a combination of surface-wave and S -wave observations (Schmid in the following).

[10] Horizontal sections through all the mentioned models with the exception of PM01 are shown in Figure 2. FB10 show that results associated with PM01 are broadly consistent with what they find from MITP08. As discussed by Boschi *et al.* [2009], tomographic models of the upper mantle under the Mediterranean Basin share the same long-wavelength pattern. Dominant features are high velocities under the east European craton, associated with deeper-than-average continental roots; a narrower high-velocity body under (and north of) the Hellenic arc, interpreted as a northward dipping subducting slab; low velocities down to ~ 200 km under the Western Mediterranean and the Aegean sea, explained by spreading activity in both regions [Wortel and Spakman, 2000]. At larger depths (~ 600 km), upper mantle structure is dominated by a system of large-scale fast heterogeneities extending from southern Iberia and the

western Mediterranean to the Alps, Carpathians, Aegean sea and Anatolia (e.g., Figure 2 of Wortel and Spakman [2000], Figure S1 of FB10), most likely related to subduction [Capitanio and Goes, 2006].

[11] Important differences are apparent at shorter scales:

[12] 1. P -velocity models are characterized by shorter-wavelength signal with respect to S -wave ones, but this might reflect the nonuniformity of body-wave data coverage, while surface waves, used to derive the S -wave models of Figure 2, sample the upper mantle more uniformly.

[13] 2. Remarkable differences between the S models of Figure 2, and the P ones employed by FB10, include a fast S heterogeneity under Adria, whose sign is inverted in the P models, and an equally strong slow heterogeneity under Iberia, not seen in the P models or in LH08.

[14] 3. The upper mantle under Anatolia is slow at 100 km depth according to Schmid, and, to some extent, LRSP30EU, in agreement with the idea of a relatively thin lithosphere; fast according to MITP08.

[15] 4. LH08 is a global model whose wavelength is by construction longer than that of the other models in Figure 2: its horizontal parameterization grid is much coarser than that of, e.g., LRSP30EU (compare Figure 5 of Lebedev and van der Hilst [2008] with Figure 2b of Boschi *et al.* [2009]).

4. Modeling

[16] We estimate mantle density structure by multiplying tomographically mapped seismic velocities by a constant scaling coefficient. For this approach to be valid, we have to assume that the effect of lateral variations in chemical composition on seismic velocities is negligible compared to that of temperature variations (FB10). The resulting 3-D density models are then input parameters of the global, finite-element code CitcomS [Zhong *et al.*, 2000], which we use (in the CIG version available at www.geodynamics.org) to model mantle flow. The other important input parameter is the assumed mantle rheology: we reproduce the preferred set-up of FB10, with (i) Newtonian viscous rheology, (ii) a 3-layer profile with viscosity equal to 10^{21} Pa \cdot s between 100 and 660 km depth, and 5×10^{22} Pa \cdot s elsewhere, and (iii) 100 km-wide, 100 km-thick surficial weak (0.01 reduction with respect to ambient viscosity) zones along main plate boundaries. FB10 verified that flow-modeled dynamic topography in this set-up is relatively insensitive to changes in rheological parameters, including lateral viscosity variations. As discussed by FB10 we prescribe the velocities of

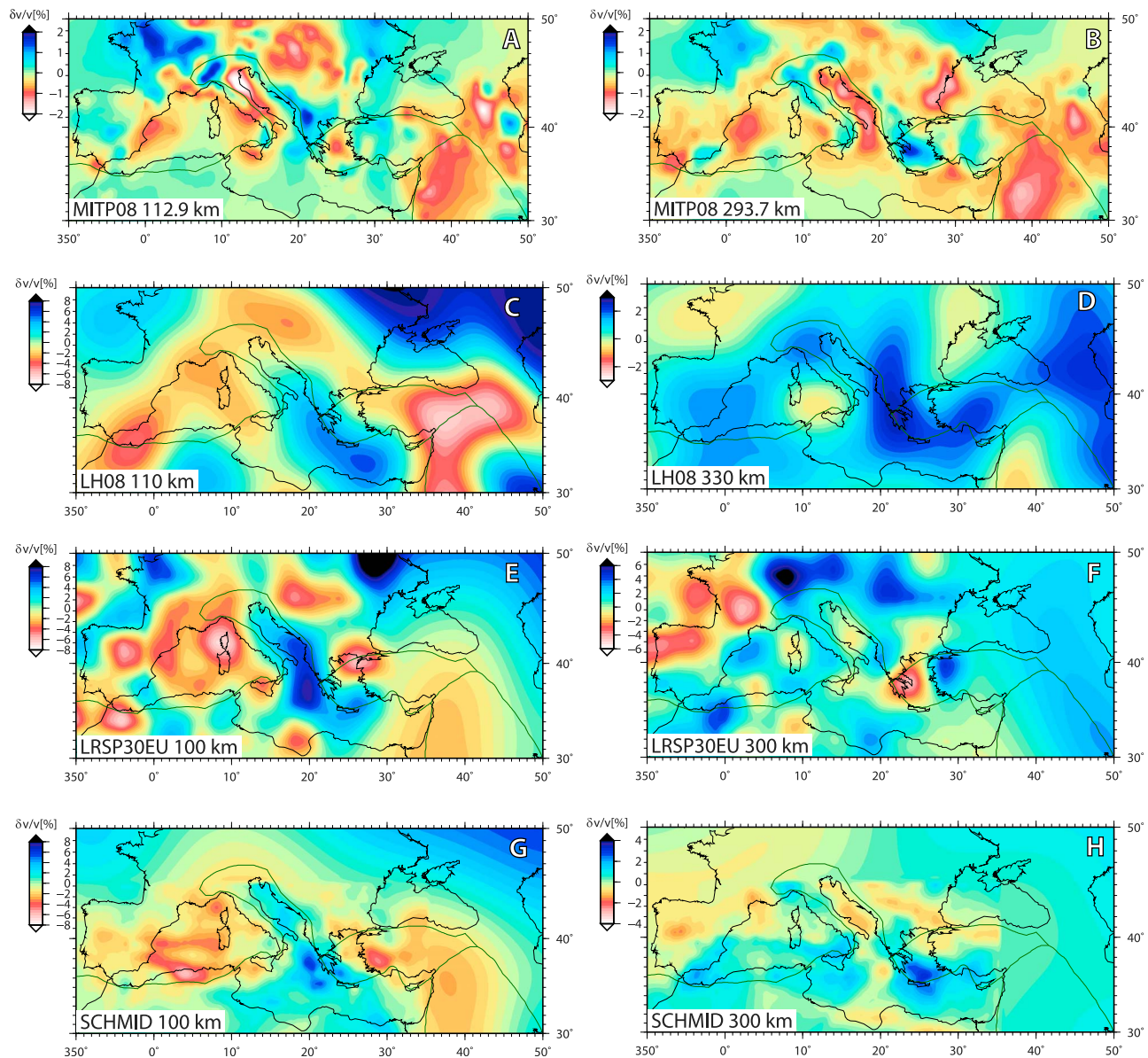


Figure 2. Horizontal sections through the tomography models described in section 3, at depths of (left) 100 and (right) 300 km below the Earth's surface. (a–d) Models already employed by FB10. (e–h) Models on which new mantle flow calculations presented here are based.

the African and Arabian plates as boundary conditions for flow computation. We do not require our flow models to fit plate velocities observed in Adria and Anatolia; these velocities are an output parameter, and we can use their similarity to corresponding GPS observations to evaluate the performance of different models.

5. Results and Discussion

[17] We show in Figure 3 the contribution of mantle flow to the surface tectonics of the Mediterranean Basin, computed on the basis of the tomography models of section 3. Comparing Figures 3 and 1, it is apparent that surface-wave based models *LH08*, *LRSP30EU* and *Schmid* achieve a better fit of observation-based estimates of dynamic

topography than the body-wave model *MITP08*. The same is true for GPS measures (yellow arrows in Figures 3b, 3d, 3f, and 3h) and dynamic predictions (white) of microplate motion. These observations are confirmed by the linear correlations between Figures 1a and 1b and modeled dynamic topography, and the mean lengths of vector difference/mean dot-products between modeled and observed velocities in Figures 3b, 3d, 3f, and 3h, given in Table 1. We explain this finding in terms of the specific properties of different tomography models. Surface waves are more sensitive than body waves to relatively shallow, upper-mantle structure; as a result, models of the upper mantle based on surface-wave data are more accurate. Because dynamic topography is mostly controlled by upper-mantle structure,

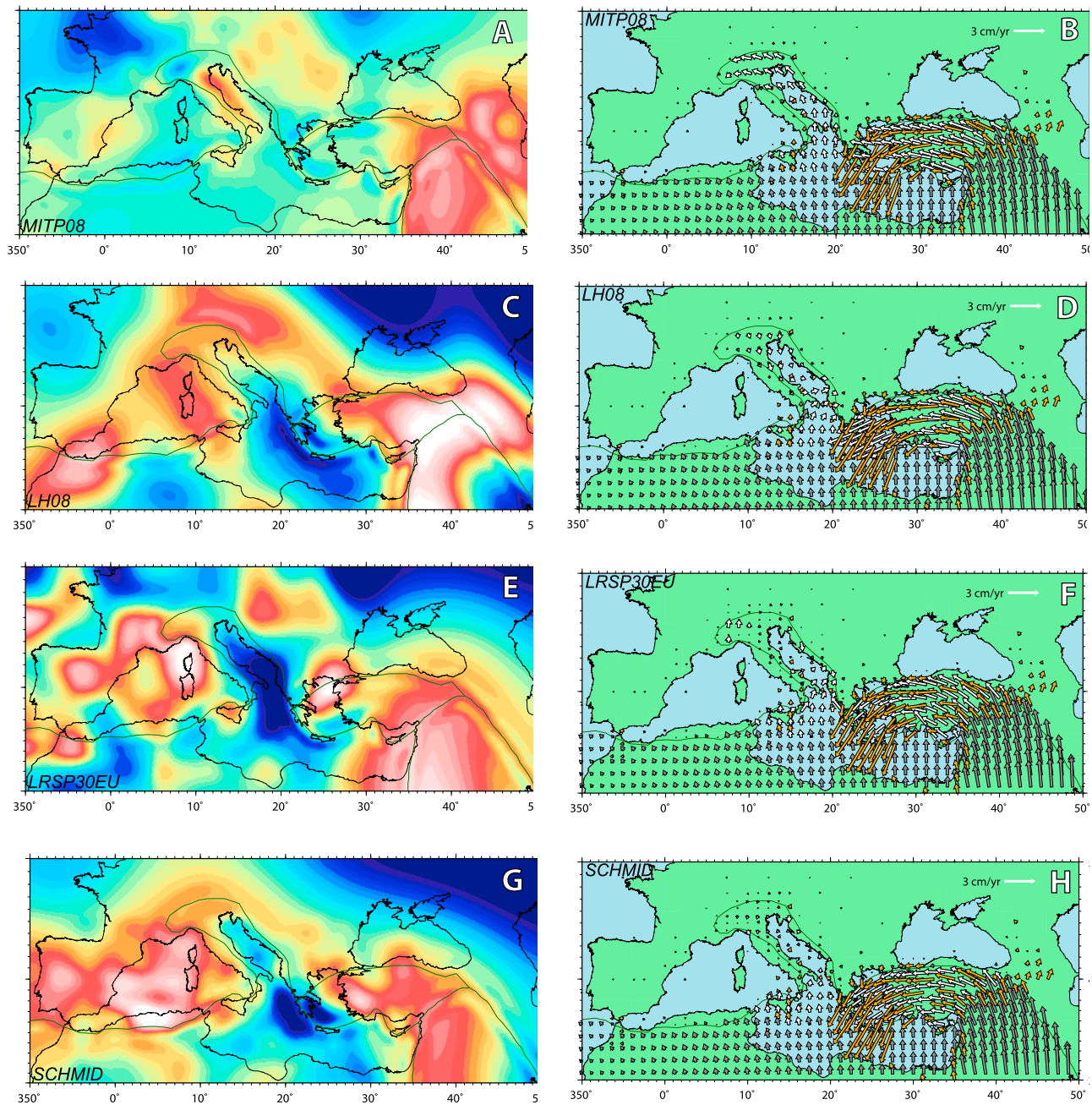


Figure 3. Maps of (a, c, e, and g) modeled dynamic topography (colour scale as in Figure 1) and (b, d, f, and h) horizontal velocity (white arrows), shown in the same order as the tomography models of Figure 2 on which they are based. GPS observations of Adria and Anatolia velocity (orange arrows), and the velocity (from NUVEL-1A) of Africa and Arabia relative to Eurasia (grey arrows) are also shown in Figures 3b, 3d, 3f, and 3h.

modeling results based on surface-wave tomography explain it best.

[18] Evaluating the comparative performance of the different S models is complicated by the difficulty inherent in correlating features of shorter spatial wavelength, at the limit of resolution for both tomography and crust models. Table 1 shows that the higher-resolution models *LRSP30EU* and *Schmid* are not improving, in comparison with *LH08*, the fit to observed dynamic topography, controlled by the longer wavelengths. Yet, *LRSP30EU* and *Schmid* are most suc-

cessful at fitting measured plate velocities. They likewise effectively predict a number of local geological features:

[19] 1. Iberia: FB10 suggest that the plateau-like morphology of the *mesetas* and alkaline volcanism can be explained in terms of mantle flow [Casas-Sainz and de Vicente, 2009]. Our new models (Figures 3e and 3g) support this idea more convincingly.

[20] 2. Massif Central: positive dynamic topography presumably related to decompression melting [Lucente *et al.*,

Table 1. Regional Linear Correlation Between the Estimates of Residual Topography Based on the Crustal Models Crust2.0 and Eurocrust07, and Dynamic Topography Computed From a Suite of *P* and *S* Tomography Results; Mean Length of Vector Differences Between Predictions and GPS Observations of Plate Velocity; and Mean Normalized Dot Product of Modeled Plate Velocities and GPS

	Crust2.0 (Corr.)	Eurocrust07 (Corr.)	GPS Data (Diff.) ^a	GPS Data (Prod.) ^b
<i>MITP08</i>	-0.03	0.01	1.04	0.74
<i>PM01</i>	0.18	0.07	1.01	0.75
<i>LH08</i>	0.56	0.38	0.93	0.80
<i>LRSP30EU</i>	0.32	0.19	0.72	0.85
<i>Schmid</i>	0.57	0.37	0.62	0.92

^aLarger values naturally correspond to worse fit.

^bNeglecting datapoints with velocity <0.3 cm/year.

2006] is a robust feature of our new models, and not of those based upon *MITP08* or *LH08*.

[21] 3. Adria: the dynamic uplift predicted in this area based on *PM01* and *MITP08* is in contrast with the observations of Figure 1. Models *LRSP30EU* and *Schmid* predict negative dynamic topography throughout Adria, in good agreement with residual topography data [Shaw and Pysklywec, 2007]. The small amplitude of Adria's horizontal motion is also predicted here more accurately than in the study of FB10, with model *LRSP30EU* also fitting, at least to some extent, its north-northeast direction.

[22] 4. Aegea: the southwestward motion of Aegea, associated with the retreat of the Hellenic slab, is reproduced in direction, if not in amplitude, by *LRSP30EU* (Figure 3f) and *Schmid* (Figure 3h).

[23] 5. Anatolia: expected positive dynamic topography in this region [Şengör et al., 2003], recovered only partially in Figures 3a and 3c, is a robust feature of our new models.

[24] Two important conclusions arise. First, after applying the method of FB10 to a larger set of tomography models, we further substantiate their conclusions: small-scale mantle flow explains the region's tectonics to an even larger extent than originally suggested. Second, surface-wave based mantle models fit observed dynamic topography and horizontal plate motions well: this confirms their reliability as reference maps of regional heterogeneity.

[25] **Acknowledgments.** All figures were generated with the Generic Mapping Tools software [Wessel and Smith, 1991]. LB is grateful to Domenico Giardini for his support and encouragement. TWB was partially supported by NSF projects MEDUSA (EAR-0633879) and PICASSO (EAR-0809023). We are thankful to all authors who shared the tomography models we discuss, to A. Morelli, S. Lebedev, F. Capitanio and anonymous reviewer for their comments and suggestions. We thank CIG and its contributors for sharing and maintaining the CitcomS software.

References

Bassin, C., G. Laske, and G. Masters (2000), Current limits of resolution for surface wave tomography in North America, *Eos Trans. AGU*, 81, F897.
 Becker, T. W., and L. Boschi (2002), A comparison of tomographic and geodynamic mantle models, *Geochem. Geophys. Geosyst.*, 3(1), 1003, doi:10.1029/2001GC000168.

Boschi, L., B. Fry, G. Ekström, and D. Giardini (2009), The European upper mantle as seen by surface waves, *Surv. Geophys.*, 30, 463–501, doi:10.1007/s10712-009-9066-2.
 Capitanio, F. A., and S. Goes (2006), Mesozoic spreading kinematics: Consequences for Cenozoic central and western Mediterranean subduction, *Geophys. J. Int.*, 165, 804–816, doi:10.1111/j.1365-246X.2006.02892.x.
 Casas-Sainz, A. M., and G. de Vicente (2009), On the tectonic origin of Iberian topography, *Tectonophysics*, 474, 214–235, doi:10.1016/j.tecto.2009.01.030.
 D'Agostino, N., A. Avallone, D. Cheloni, E. D'Anastasio, S. Mantenuto, and G. Selvaggi (2008), Active tectonics of the Adriatic region from GPS and earthquake slip vectors, *J. Geophys. Res.*, 113, B12413, doi:10.1029/2008JB005860.
 Daradich, A., J. X. Mitrovica, R. N. Pysklywec, S. D. Willett, and A. M. Forte (2003), Mantle flow, dynamic topography, and rift-flank uplift of Arabia, *Geology*, 31, 901–904, doi:10.1130/G19661.1.
 DeMets, C., R. G. Gordon, D. F. Argus, and S. Stein (1990), Current plate motions, *Geophys. J. Int.*, 101, 425–478, doi:10.1111/j.1365-246X.1990.tb06579.x.
 DeMets, C., R. G. Gordon, D. F. Argus, and S. Stein (1994), Effect of recent revisions to the geomagnetic reversal time-scale on estimates of current plate motions, *Geophys. Res. Lett.*, 21, 2191–2194, doi:10.1029/94GL02118.
 Faccenna, C., and T. W. Becker (2010), Shaping mobile belts by small-scale convection, *Nature*, 465, 602–605, doi:10.1038/nature09064.
 Favali, P., R. Funicello, G. Mattiotti, G. Mele, and F. Salvini (1993), An active margin across the Adriatic Sea (central Mediterranean Sea), *Tectonophysics*, 219, 109–117, doi:10.1016/0040-1951(93)90290-Z.
 Ferranti, L., et al. (2006), Markers of the last interglacial sea-level high stand along the coast of Italy: Tectonic implications, *Quat. Int.*, 145–146, 30–54, doi:10.1016/j.quaint.2005.07.009.
 Forte, A. M. (2007), Constraints on seismic models from other disciplines: Implications for mantle dynamics and composition, in *Treatise on Geophysics*, vol. 1, *Seismology and the Structure of the Earth*, edited by B. Romanowicz and A. M. Dziewonski, pp. 805–858, doi:10.1016/B978-044452748-6.00027-4, Elsevier, Amsterdam.
 Gurnis, M. (2001), Sculpting the Earth from inside out, *Sci. Am.*, 284, 40–47, doi:10.1038/scientificamerican0301-40.
 Lebedev, S., and R. D. van der Hilst (2008), Global upper-mantle topography with the automated multimode inversion of surface and *S*-wave forms, *Geophys. J. Int.*, 173, 505–518, doi:10.1111/j.1365-246X.2008.03721.x.
 Li, C., R. D. van der Hilst, E. R. Engdahl, and S. Burdick (2008), A new global model for *P* wave speed variations in Earth's mantle, *Geochem. Geophys. Geosyst.*, 9, Q05018, doi:10.1029/2007GC001806.
 Lithgow-Bertelloni, C., and P. G. Silver (1998), Dynamic topography, plate driving forces and the African superswell, *Nature*, 395, 269–272, doi:10.1038/26212.
 Lucente, F. P., L. Margheriti, C. Piromallo, and G. Barruol (2006), Seismic anisotropy reveals the long route of the slab through the western-central Mediterranean mantle, *Earth Planet. Sci. Lett.*, 241, 517–529, doi:10.1016/j.epsl.2005.10.041.
 Moucha, R., A. M. Forte, J. X. Mitrovica, D. B. Rowley, S. Quere, N. A. Simmons, and S. P. Grand (2008), Dynamic topography and long-term sea-level variations: There is no such thing as a stable continental platform, *Earth Planet. Sci. Lett.*, 271, 101–108, doi:10.1016/j.epsl.2008.03.056.
 Piromallo, C., and A. Morelli (2003), *P* wave tomography of the mantle under the Alpine-Mediterranean area, *J. Geophys. Res.*, 108(B2), 2065, doi:10.1029/2002JB001757.
 Reilinger, R., et al. (2006), GPS constraints on continental deformation in the Africa-Arabia-Eurasia continental collision zone and implications for the dynamics of plate interactions, *J. Geophys. Res.*, 111, B05411, doi:10.1029/2005JB004051.
 Ritsema, J., H. J. van Heijst, and J. H. Woodhouse (1999), Complex shear wave velocity structure imaged beneath Africa and Iceland, *Science*, 286, 1925–1928, doi:10.1126/science.286.5446.1925.
 Schmid, C., S. van der Lee, J. C. VanDecar, E. R. Engdahl, and D. Giardini (2008), Three-dimensional *S* velocity of the mantle in the Africa-Eurasia plate boundary region from phase arrival times and regional waveforms, *J. Geophys. Res.*, 113, B03306, doi:10.1029/2005JB004193.
 Şengör, A. M. C., S. Özeren, T. Genç, and E. Zor (2003), East Anatolian high plateau as a mantle-supported, north-south shortened domal structure, *Geophys. Res. Lett.*, 30(24), 8045, doi:10.1029/2003GL017858.
 Serpelloni, E., G. Vannucci, S. Pondrelli, A. Argnani, G. Casula, M. Anzidei, P. Baldi, and P. Gasperini (2007), Kinematics of the western Africa-Eurasia plate boundary from focal mechanisms and GPS data, *Geophys. J. Int.*, 169, 1180–1200, doi:10.1111/j.1365-246X.2007.03367.x.
 Shaw, M., and R. Pysklywec (2007), Anomalous uplift of the Apennines and subsidence of the Adriatic: The result of active mantle flow?, *Geophys. Res. Lett.*, 34, L04311, doi:10.1029/2006GL028337.

- Tesauro, M., M. K. Kaban, and S. A. P. L. Cloetingh (2008), EuCRUST-07: A new reference model for the European crust, *Geophys. Res. Lett.*, *35*, L05313, doi:10.1029/2007GL032244.
- Wessel, P., and W. H. F. Smith (1991), Free software helps map and display data, *Eos Trans. AGU*, *72*(41), 441, doi:10.1029/90EO00319.
- Wortel, M. J. R., and W. Spakman (2000), Subduction and slab detachment in the Mediterranean-Carpathian region, *Science*, *290*, 1910–1917, doi:10.1126/science.290.5498.1910.
- Zhong, S. J., M. T. Zuber, L. Moresi, and M. Gurnis (2000), Role of temperature-dependent viscosity and surface plates in spherical shell models of mantle convection, *J. Geophys. Res.*, *105*, 11,063–11,082, doi:10.1029/2000JB900003.
-
- T. W. Becker, Department of Earth Sciences, University of Southern California, MC 0740, Los Angeles, CA 90089-0740, USA.
- L. Boschi, Institute of Geophysics, ETH, Sonneggstrasse 5, CH-8092 Zürich, Switzerland. (larryboschi@gmail.com)
- C. Faccenna, Dipartimento di Scienze Geologiche, Università di Roma 3, Largo San Leonardo Murialdo 1, I-00146 Roma, Italy.